Chirping in Plasmas; test of criterion for chirping onset & simulation of explosive chirping

H. L. Berk, B. N. Breizman (presenter), G. Wang, L. Zheng;
University of Texas at Austin, Austin, Texas 78723, USA
V.N. Duarte[1], N. N. Gorelenkov, G. Kramer, N. Nazikian, M. Podesta, B. J. Tobias;
Princeton Plasma Physics Laboratory, Princeton, N.J. 08543, USA
W. W. Heidbrink;
University of California Irvine; Irvine, CA, 92697 USA
D.C. Pace, M.A. Van Zeeland;
General Atomics, San Diego 92186 CA USA

[1]. also University of São Paulo, Brazil

Introduction
Predicting and understanding frequency chirping in fusion experiments

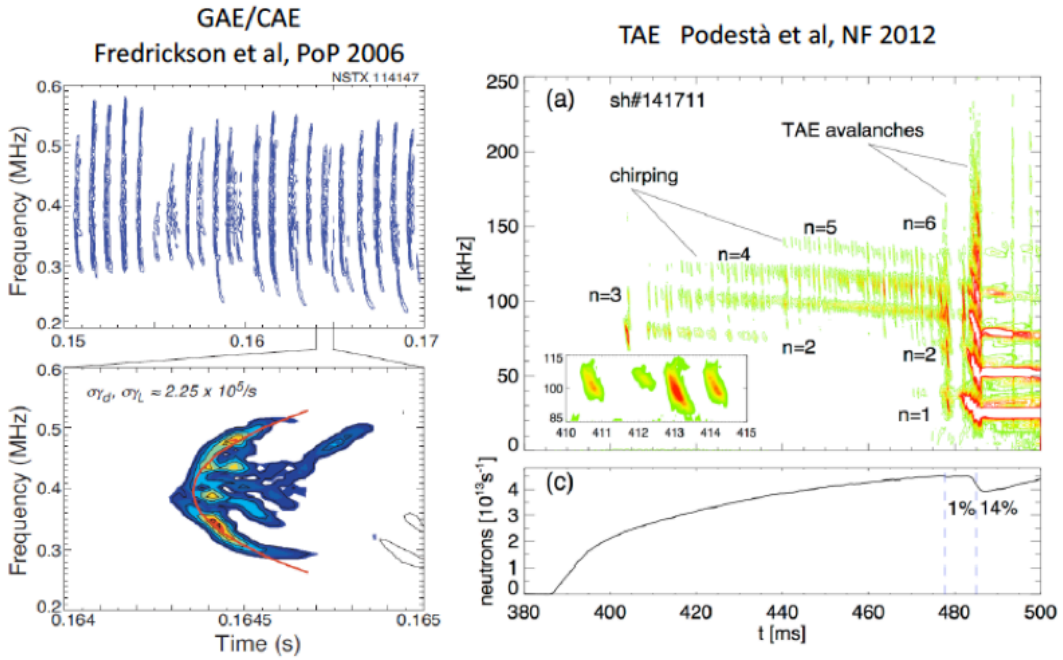

1. Spontaneous fast chirping phenomena is often observed in experiments with energetic particles that excite Alfvenic instabilities. Above are examples in NSTX
2. NSTX experiments frequently observes chirping, while chirping is rarely observed in DIII-D. Why?
3. Here we use an expanded version of a theoretical model, (first proposed by Lilley, Sharapov and Breizman, (2009)) to see if a predictive theory can be employed to explain, when there is Alfvenic instablity, whether chirping will or will not arise.
4. The above figure on right, of NSTX data, shows that TAE modes can increase in intensity with time, and even produce rapid and large frequency shift chirping events.
5. Here we show a numerical simulation of this rapid chirping mechanism using a reduced simulation theory for TAE modes that replicates some of the important features of the chirping response.

Nonlinear dynamics of driven kinetic systems close to threshold

Starting point: **kinetic equation** plus **wave equation**

Assumptions:

- Perturbative procedure for expansion in mode amplitude
- Truncation at third order due to closeness to marginal stability
- First use characteristic parameter to obtain problem identical to bump-on-tail

Cubic equation: lowest-order nonlinear correction to the evolution of mode amplitude A:

(Hickernell, 1982 (fluids), Berk, Breizman and Pekker, PRL 1996 Lilley, Breizman and Sharapov, PRL 2009)

$$\frac{dA}{dt} = A - \int_0^{t/2} d\tau \tau^2 A(t-\tau) \int_0^{t-2\tau} d\tau_1 e^{-\nu_{scatt}^3 \tau^2 (2\tau/3+\tau_1) + i\nu_{drag}^2 \tau(\tau+\tau_1)} A(t-\tau-\tau_1) A^*(t-2\tau-\tau_1)$$

Predicts a sufficient condition for onset of chirping: when no stationary response exists

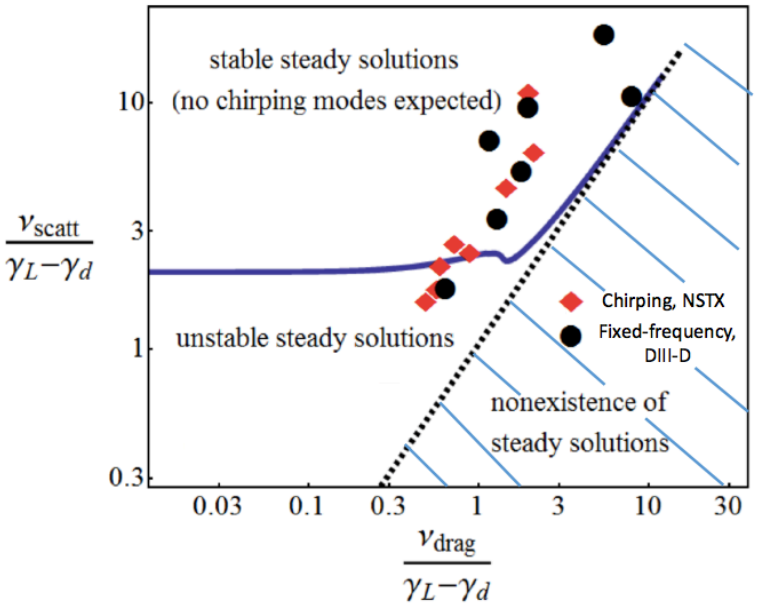

- First Attempt (use characteristic parameters).
- Dashed line separates blank and hatched regions.
- In hatched region no steady solutions exist where Vlasov simulations have always produced chirping.
- In blank region there always is a steady solution (though steady solution can be unstable).
- Unstable region below solid curve has rather complicated response. Nonetheless, dotted line roughly separates chirping and steady regions.
- Criterion most reliable in upper right regions.
- This prediction not good for NSTX; marginal for DIII-D

How better comparison with experiment is obtained

1. Accurate theory requires determination of eigenfunction's spatial profile
2. Include phase space dependence of the physical quantities;
   the stochastic diffusion due to both pitch angle scattering
   and **background turbulent diffusion** (not previously considered in this problem)

$$\int_0^{t/2} d\tau \tau^2 A(t-\tau) \int_0^{t-2\tau} d\tau_1 \, \mathrm{e}^{-v_{stoch}^3(2\tau/3+\tau_1)+iv_{drag}^2(\tau+\tau_1)} A(t-\tau-\tau_1)A^*(t-2\tau-\tau_1) \rightarrow$$

$$\int_0^{t/2} d\tau \tau^2 A(t-\tau) \sum_{\sigma_{\|},\mathrm{j}} \int dE \, d\mu \frac{\tau_b}{\nu_{stoch,n,j}^4} |V_{n,j}|^4 \left| n^2 \frac{\partial \Omega_{n,j}}{\partial P_\phi} \right|_{E'} \left| Int(E, P_\phi(E,\mu),\mu) \frac{\partial F}{\partial P_\phi} \right|_{E'=E-\omega P_\phi/n} \times$$

$$\int_0^{t-2\tau} d\tau_1 \, \mathrm{e}^{-v_{stoch}^3(2\tau/3+\tau_1)+iv_{drag}^2(\tau+\tau_1)} A(t-\tau-\tau_1)A^*(t-2\tau-\tau_1)$$

where the stochastic diffusion term v_{stoch}^3, the electron drag term v_{drag}^2,

and the wave interaction term $|V_{n,j}|^4$ are functions in phase space at

phase space points, $(E, P_\phi(E,\mu),\mu)$ which is determined from the relation:

$$\Omega_{n,j}(E,\mu) \equiv n\omega_\phi\left(E, P_\phi(E,\mu),\mu\right) + j\omega_\theta\left(E, P_\phi(E,\mu),\mu\right) = \omega,$$

and $\left.\frac{\partial}{\partial P_\phi}\right|_{E'=E-\omega P_\phi/n} \equiv \left(\frac{\partial}{\partial P_\phi} + \frac{\omega}{n}\frac{\partial}{\partial E}\right) \equiv \frac{1}{n}\frac{\partial}{\partial I};$ The important function *Int* is discussed in the next slide

A general criterion for Alfvén wave chirping

(strongly dependent on competition between fast ion scattering and drag)

$$Crt = \frac{1}{N}\sum_{j,\sigma_{\|}} \int dP_{\varphi} \int d\mu \frac{|V_j|^4}{\omega_{\theta}\nu_{drag}^4} \left|\frac{\partial \Omega_j}{\partial I}\right| \frac{\partial f}{\partial I} Int$$

>0: fixed-frequency likely

<0: chirping likely

$$Int \equiv Re \int_0^{\infty} dz \frac{z}{\frac{\nu_{stoch}^3}{\nu_{drag}^3} z - i} exp\left[-\frac{2}{3}\frac{\nu_{stoch}^3}{\nu_{drag}^3} z^3 + iz^2\right]$$

Crt accounts for collisional coefficients varying along resonances and particle orbits

Phase space integration

Resonance surfaces:

$$\Omega_j\left(E' + \omega I, nI, \mu\right) =$$
$$n\omega_{\phi}\left(E' + \omega I, nI, \mu\right) + j\omega_{\theta}\left(E' + \omega I, nI, \mu\right) - \omega$$

Eigenstructure information:

$$q \int dt \mathbf{v}_{dr} \cdot \delta \mathbf{E} e^{i\omega t}$$

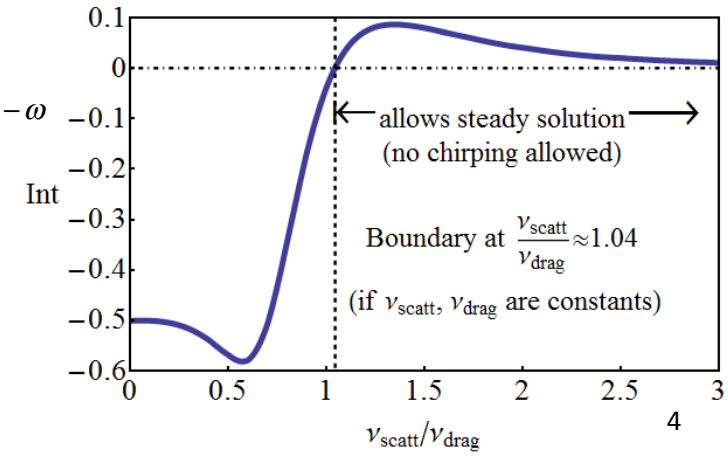

Criterion was incorporated into NOVA-K: nonlinear prediction from linear physics elements

Turbulence scattering explains why chirping common in NSTX but rare in DIII-D

Proposed criterion for *Alfvén wave* chirping onset:

Duarte, Berk, Gorelenkov *et al*, PRL (submitted)

$$Crt = \frac{1}{N}\sum_{j,\sigma_{\|}} \int dP_{\varphi} \int d\mu \frac{|V_j|^4}{\omega_{\theta}\nu_{drag}^4} \left|\frac{\partial \Omega_j}{\partial I}\right| \frac{\partial f}{\partial I} Int$$

>0: fixed-frequency likely

<0: chirping likely

Inclusion of fast ion micro-turbulence

From GTC gyrokinetic simulations for passing particles (Zhang, Lin and Chen, PRL 2008):

$$D_{EP}\left(E_{EP}\right) \approx D_{th,i}\frac{5T_e}{E_{EP}}$$

Unlike in DIII-D, ion transport in NSTX in mostly neoclassical

chirping, NSTX

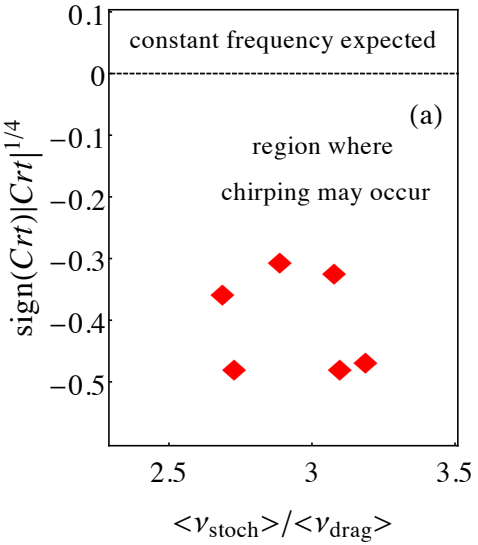

Fixed-frequencies, DIII-D and TFTR

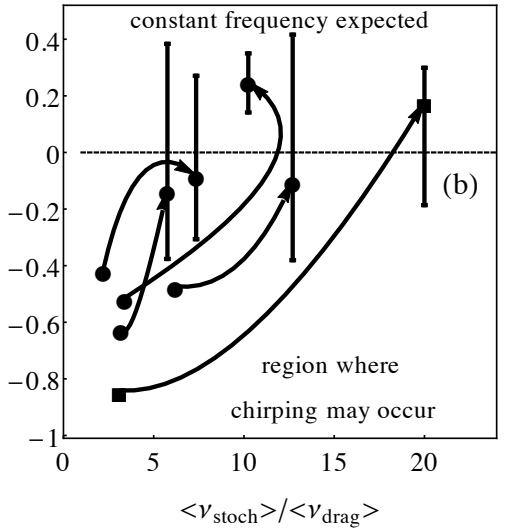

In NSTX , Alfvén wave chirping criterion agrees with experimental Data. Criterion value insensitive to ~ 30% increase in $\langle \nu_{stoch} \rangle$ due to micro-turbulence.

Arrows indicate shift in chirping criterion in going from $\langle \nu_{stoch} \rangle$ due to pitch angle scattering alone, to due to micro-turbulence and pitch-angle scattering

Correlation between the emergence of chirping and a substantial decrease of ion micro-turbulence in DIII-D:

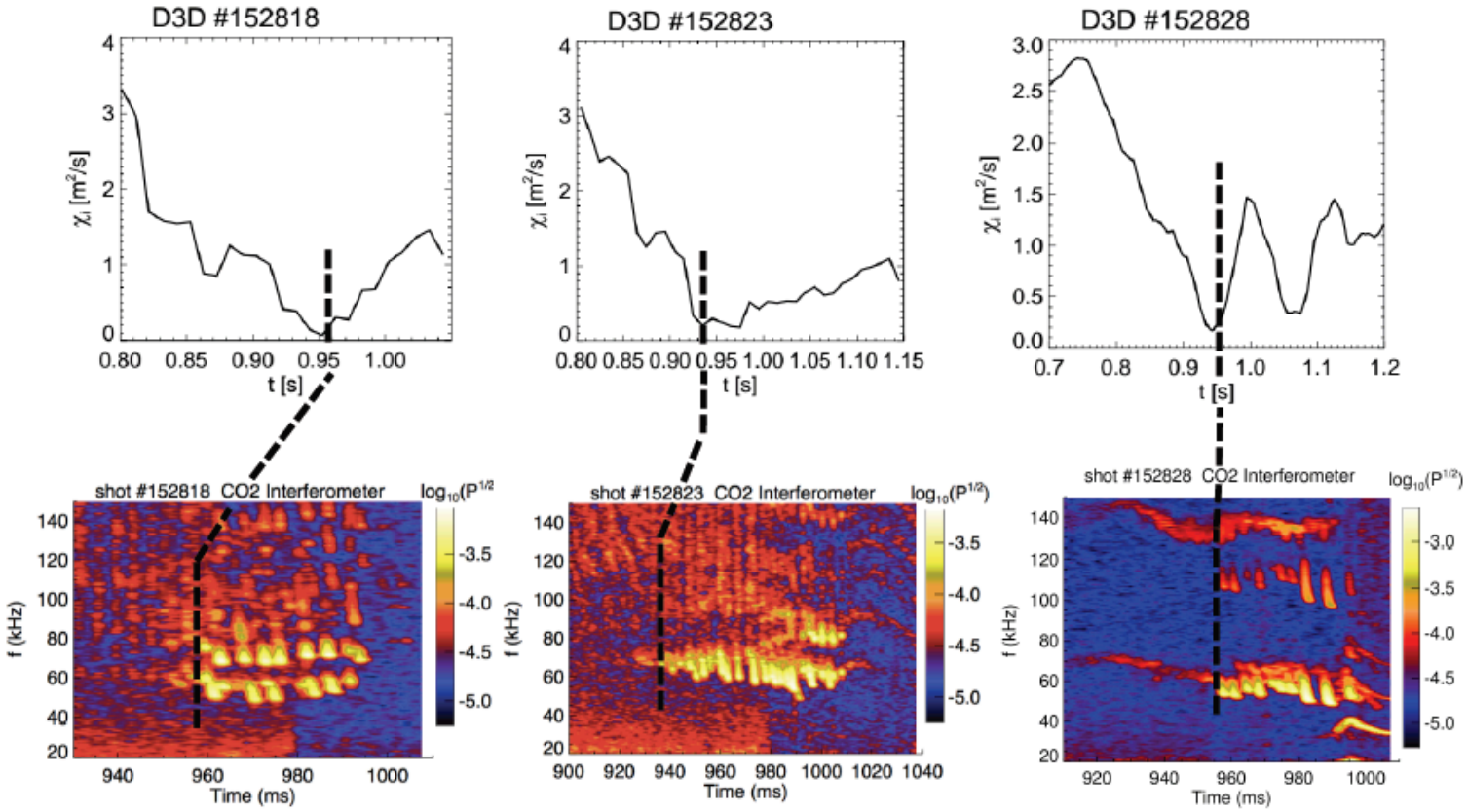

DIII-D data does not typically show fast chirping. When such chirping does arise, it occurs when micro-turbulent transport is reduced, prior to L-H transition, as is displayed in above figures.

Conclusions

1. A theoretical criterion for chirping onset of TAE modes in experiment was compared with experimental data in NSTX and DIII-D.
2. Very good correlation was obtained between the two only when the theory incorporated the correct profiles for the mode structure, the dependence of velocity diffusion on pitch angle scattering and the inclusion of energetic particle diffusion due to background turbulence, taking into account the reduction of energetic particle diffusion with energy due to FLR averaging over rapidly spatially varying turbulent structures.
3. NSTX data displayed a strong tendency for chirping in agreement with theoretical predictions, as background ion transport, which is low (it is neo-classical) so that classical pitch-angle scattering is the main contributor to the diffusive process, and this diffusion is not strong enough to prevent the onset of chirping of TAE modes.
4. Most DIII-D shots produced steady oscillations during Alfvenic instability. In these shots the background turbulence appeared large enough to prevent chirping from arising.
5. Only a small minority of DIII-D shots produced a chirping response. It was found that on these shots there was a pronounced reduction in the background ion-turbulence level.
6. This investigation appears to have answered a previous puzzle for why, when Alfvenic oscillations appear in experimental data in NSTX and DIII-D, chirping Alfvenic modes usually arise in NSTX but only rarely arise in DIII-D.
7. This method of analysis can be applied to other experiments including ITER.

TAE Podestà et al, NF 2012

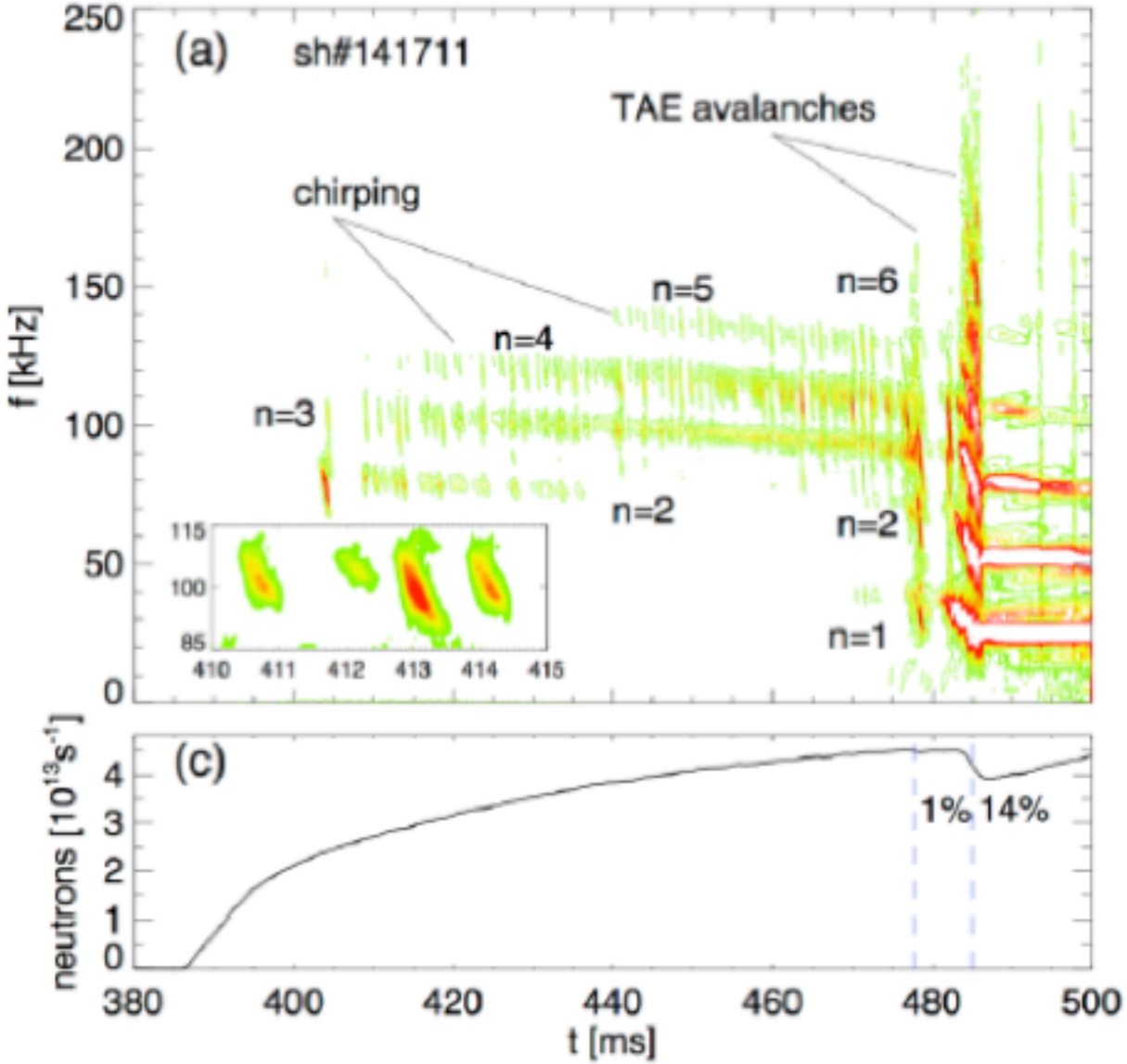

Build simulation code based on perturbation from equilibrium orbits

- Advantage: Time step not based on mode frequency but on strength of wave particle interaction
- Wave equation based on modification of WKB method:

$$\frac{\partial^2}{\partial t^2} \leftrightarrow -\omega^2(t) - i2\omega(t)\frac{\partial}{\partial t}$$

- For test case we treat large aspect $1/\varepsilon = R/r \approx v_{//}^2 / v_{\perp}^2 \varepsilon >> 1$ and circular tokamak geometry
- We derive an inner region wave equation, that can be matched to a fixed out region solution (manner similar to Δ' matching of tearing modes).
- Currents in wave equation assumed generated by a particle response to a Hamiltonian with a single slowly varying frequency component

Inner region wave equation and current

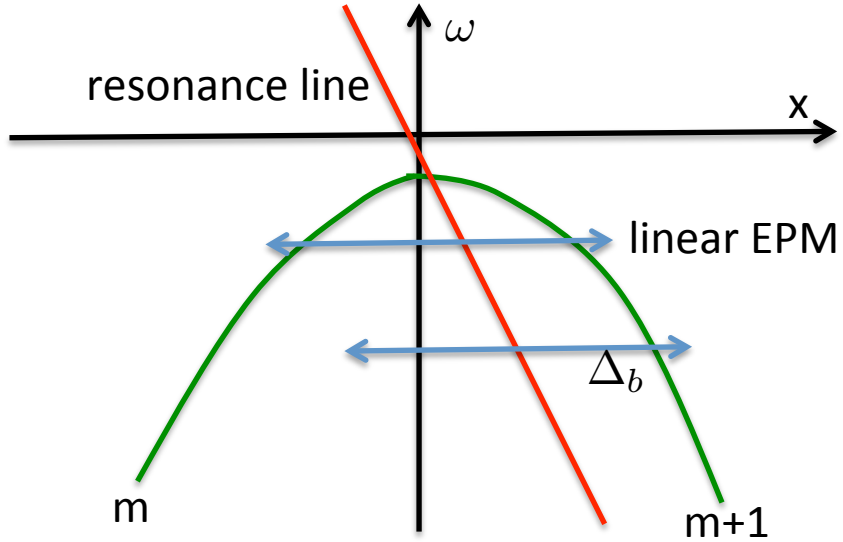

- Wave trapped EP's move along resonance line:

$$\Omega(x) = \frac{nv_{\|}}{R} - \frac{(m+l)v_{\|}}{q(x)R} - \omega(t)$$

- Linear EPM becomes unstable near the low tip with the EP orbits penetrating both continuum points.

$$(\omega(t) + 1 + \imath\frac{\partial}{\partial t})\psi^{+}(x,t) - x\psi^{-}(x,t) = -C^{-}(t) + J^{+}(x,t)$$

$$(\omega(t) - 1 + \imath\frac{\partial}{\partial t})\psi^{-}(x,t) - x\psi^{+}(x,t) = -C^{+}(t) + J^{-}(x,t)$$

where the current source terms cause the resonant interaction between EPs and waves:

$$J^{+}(x,t) = \eta\beta_{EP}\int_0^{\pi} d\theta \int_0^{2\pi} d\xi e^{-\imath\xi} f(\xi, x - \Delta_b\cos\theta, t)(\cos(l+1)\theta + \cos l\theta - \cos(l-1)\theta - \cos(l-2)\theta)$$

$$J^{-}(x,t) = \eta\beta_{EP}\int_0^{\pi} d\theta \int_0^{2\pi} d\xi e^{-\imath\xi} f(\xi, x - \Delta_b\cos\theta, t)(\cos(l+1)\theta - \cos l\theta - \cos(l-1)\theta + \cos(l-2)\theta)$$

Reduced Vlasov Equation

Bounce averaged drift-kinetic equation:

$$\frac{\partial f}{\partial t} + [f, \mathcal{H}] = 0$$

where in the wave frame the Hamiltonian is obtained: (below Δ_Ω normalized orbit width)

$$\mathcal{H}(\xi,\Omega) = \frac{\Omega^2}{2} + \lambda \Re[e^{\imath\xi} \int_0^\pi d\theta(\cos(l+1)\theta + \cos l\theta - \cos(l-1)\theta - \cos(l-2)\theta)\psi^+(\Omega + \Delta_\Omega \cos\theta)$$
$$+(\cos(l+1)\theta - \cos l\theta - \cos(l-1)\theta + \cos(l-2)\theta)\psi^-(\Omega + \Delta_\Omega \cos\theta)] + \frac{d\omega}{dt}\xi$$

Wave and Vlasov equations are solved together. As an example for EPM mode, we see phase space clump structure in the wave frame and comparison of separatrix shape between simulation and theory.

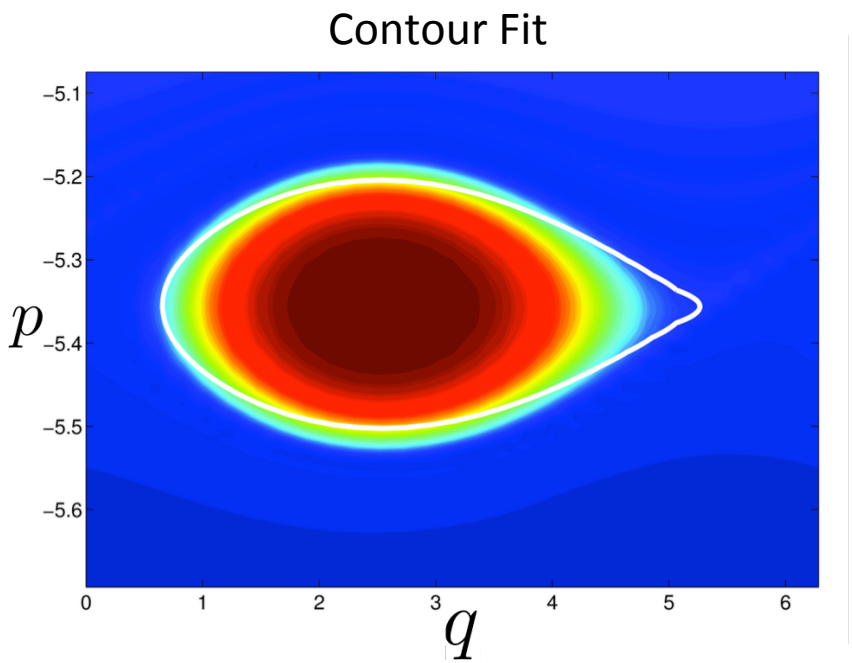

Linear EPM mode

Linear unstable TAE and EPM mode are calculated using a non-perturbative linear eigenmode code. EPM mode emerges in continuum at threshold n_h/n_0.

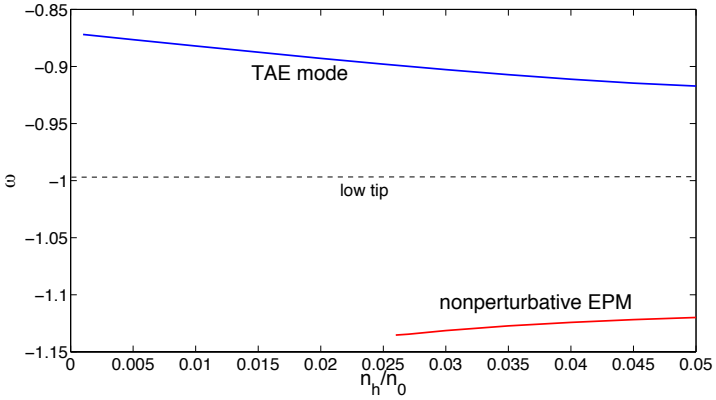

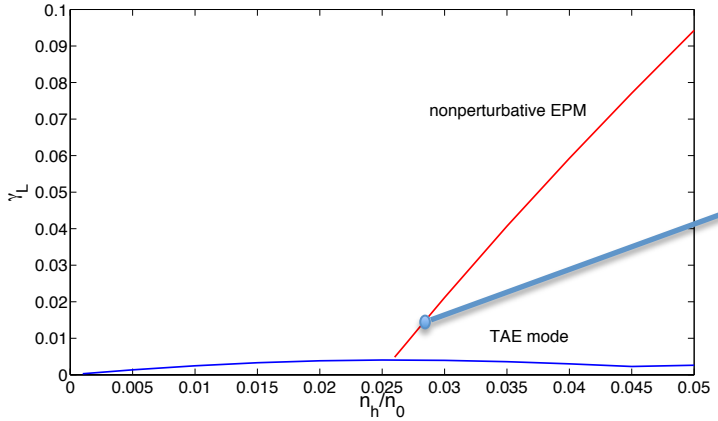

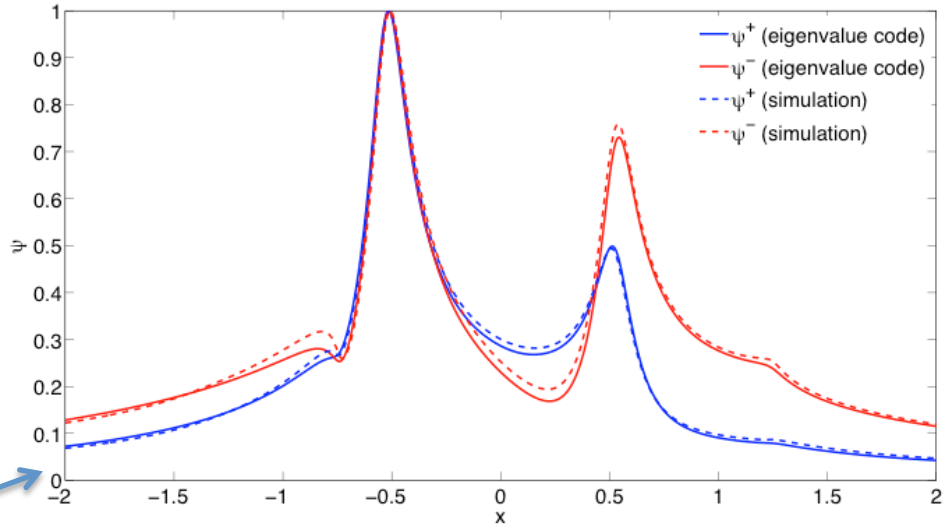

Result from simulation

- Long period of limited benign chirping, then converting to EPM mode;
- Upon EPM excitation, rapid downward chirp that propagates through continuum, until model no longer valid.

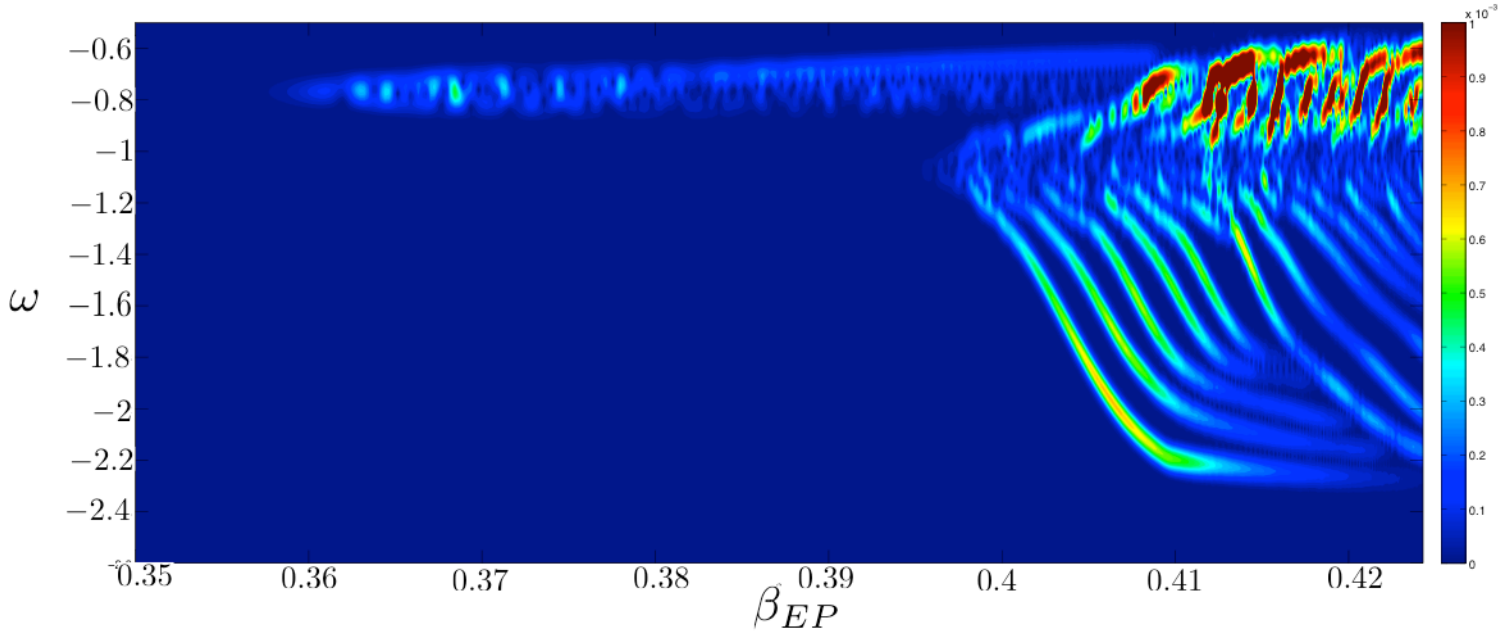

Note that rapid chirp appears on time scale comparable to physically observed time scale.

Simulation estimate of chirp rate in several MHz/s range as in experiment

Simplified nonlinear stage predictions of EPM compared to simulation

Complex amplitude, $\psi_{m+1}\left(x,\omega(t);\omega_b^2,\frac{d\omega}{dt}\right)\equiv\frac{1}{2}\left(\psi^+-\psi^-\right)$ solved by stationary phase method

Distribution $f(\xi,\Omega,t)=f(J(t))$ determined by assuming adiabaticity conservation of wave trapped particles and with adiabatic entrapment of passing particles with increasing separatrix.

We obtain following expression. LHS real, RHS complex in general with reality imposed.

$$\omega_b^2(\Omega=0,\omega)=G(\omega_b,\frac{d\omega}{dt},\omega)=\lambda\int_0^\pi d\theta\sin^2\theta\psi_m(\omega(t)+\Delta_\Omega\cos\theta)$$

Now we solve for $\left(\omega_b,\alpha(t)\equiv\omega_b^{-2}d\omega(\mathrm{t})/dt\right)$ vs. $\omega(\mathrm{t})$ and compare with simulation solution:

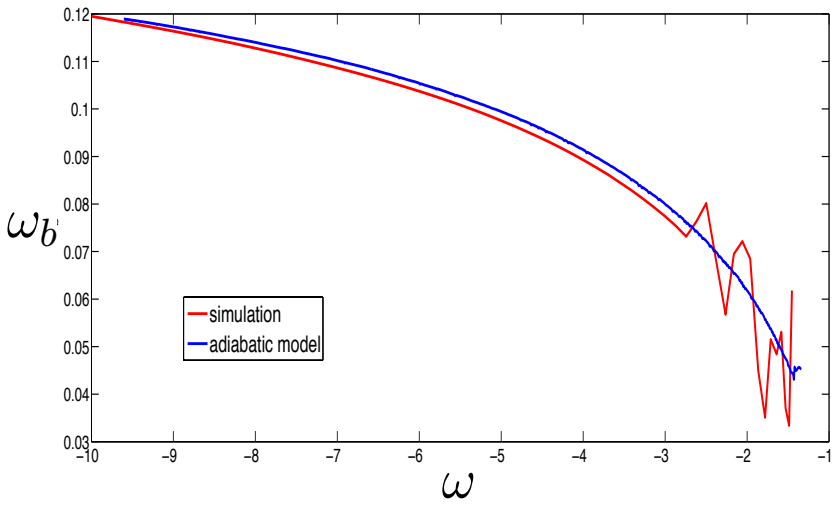

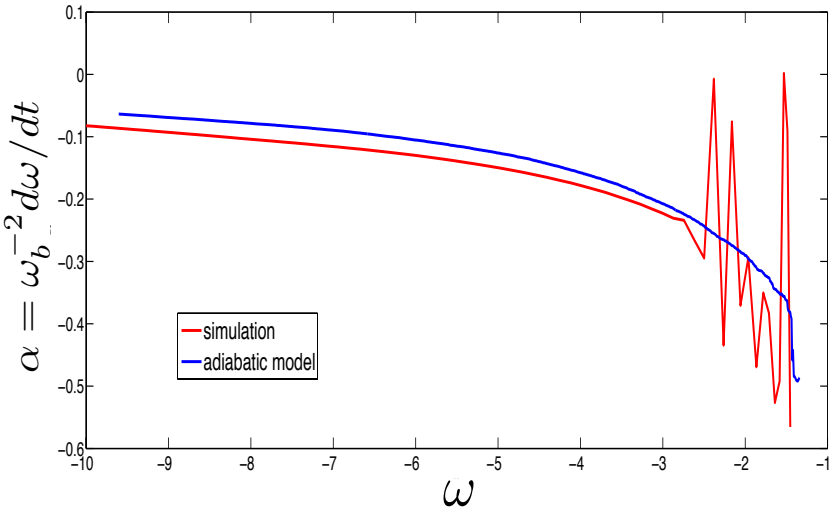

Conclusion & Comments

- Proof of principle for viability of method. Allows simulation simplification that serves as guide to theoretical analysis
- Important physical mechanism clarified: How explosive chirping can emerge and with the maintenance of adiabaticity during chirp.
- MHD nonlinearity absent in this presentation. Experimental data, showing locking of mode frequencies at several n-values, indicative for need of accounting for MHD non-linearity to achieve better theoretical modeling.
- Future work needs to generalize method to when equilibrium guiding center orbits have more general properties than being displaced circles.
- Challenge to develop efficient transformation and inverse transformation from action angle frame of particles to field coordinate variables

FINIS